Biomaterials Science

ROYAL SOCIETY OF CHEMISTRY

PAPER

View Article Online
View Journal | View Issue

Cite this: *Biomater. Sci.*, 2023, **11**, 4032

Electrospun polymer fibers modified with FK506 for the long-term treatment of acute cardiac allograft rejection in a heart transplantation model

Cheng Deng,†[a,b,c] Qiaofeng Jin,†[a,b,c] Jia Xu,[a,b,c] Wenpei Fu,[a,b,c] Mengrong He,[a,b,c] Lingling Xu,[a,b,c] Yishu Song,[a,b,c] Wenyuan Wang,[a,b,c] Luyang Yi,[a,b,c] Yihan Chen,[a,b,c] Tang Gao,[a,b,c] Jing Wang,[a,b,c] Qing Lv,[a,b,c] Yali Yang,[a,b,c] Li Zhang*[a,b,c] and Mingxing Xie *[a,b,c]

FK506, a first-line immunosuppressant, is routinely administered orally and intravenously following heart transplantation. However, frequent administration can result in a substantial psychological burden to patients, resulting in non-adherence to medication. The purpose of our study is to overcome the disadvantages of systemic drug administration by developing a polymer-based delivery system that is tunable and biodegradable and that can release highly hydrophobic FK506 over extended periods to treat or prevent acute cardiac allograft rejection. Using an electrospinning method, long-acting microfibers were prepared, and FK506 appeared to be continuously released for up to 14 days based on the *in vitro* release profiles. After implanting the microfiber subcutaneously into the abdominals of transplanted rats, it was found that the infiltration of T cells and macrophages and the secretion of interleukin-2 (IL-2) and IL-1β were significantly reduced compared with those of the free FK506 groups. More importantly, the mean survival time (MST) of the PCL-FK506 group was significantly extended in comparison with that of untreated control recipients and free FK506 (MST of untreated control recipients, free FK506, and PCL-FK506 was 8, 26.1, and 37, respectively). In conclusion, we propose that this drug delivery approach would be suitable for developing long-lasting immunomodulatory agents that prolong cardiac graft survival safely and effectively.

Received 2nd March 2023,
Accepted 17th April 2023

DOI: 10.1039/d3bm00374d

rsc.li/biomaterials-science

1 Introduction

Heart transplantation is the definitive treatment for patients with advanced heart failure.[1] Patients need to take immunosuppressants, like FK506 or CsA, to prevent acute rejection after transplantation. However, frequent administration is a substantial psychological burden to patients, contributing to an incidence of medication nonadherence, and it often greatly influences effective therapy and outcomes.[2] Therefore, long-acting drug delivery systems, widely used to deliver drugs over a long period, have been considered an attractive solution.[3] These formulations can achieve release profiles from days to months and improve patient adherence.[4,5] Notably, antipsychotic drugs and steroidal hormones have been successfully commercialized as long-acting therapeutic alternatives.[6] However, there are still some troubles in constructing long-acting drug delivery systems.

Fortunately, new advanced techniques in drug delivery have emerged to overcome some of the obstacles and limitations of long-acting formulations, like nanotechnology, 3D printing, and electrospinning.[7] Specifically, electrospinning has emerged as a powerful technique to produce fibrous structures, and it is a simple and efficient method for preparing long-acting formulations.[8–10] It applies a high voltage to spray charged threads of the drug-loaded polymer solution and results in nano/microfibers on solvent evaporation.[11] Recently, various electrospinning drug delivery systems have been prepared for the local delivery of therapeutic agents owing to the ease of drug encapsulation and high versatility in drug formulations.[12,13] It has also shown great potential in tissue engineering, regenerative medicine, tumor treatment, skin repair and antibacterial fields.[14,15]

In recent years, polycaprolactone (PCL) has been used extensively for electrospinning to deliver drugs. Various dosage

[a]*Department of Ultrasound Medicine, Union Hospital, Tongji Medical College, Huazhong University of Science and Technology, Wuhan 430022, China. E-mail: zli429@hust.edu.cn, xiemx@hust.edu.cn*
[b]*Hubei Province Clinical Research Center for Medical Imaging, Wuhan, 430022, China*
[c]*Hubei Province Key Laboratory of Molecular Imaging, Wuhan, 430022, China*
†These authors contributed equally to this work.

forms have been developed, including patches, implants, and films.[16–19] The PCL films fabricated by electrospinning are highly porous, have high surface-to-volume ratios, and have excellent mechanical properties, making them a suitable choice for biomedical applications.[20,21] PCL film-based long-acting drug delivery systems have been widely used to treat chronic diseases like diabetes, cancer, and brain disorders.[22–24] Hence, we hypothesize that PCL-based nano/microfibers can be used to deliver immunosuppressants for treating acute cardiac allograft rejection.

FK506, a widely used immunosuppressive agent, has achieved great progress in heart transplantation. Our group recently introduced a sustained-release formulation of FK506 for treating acute cardiac allograft rejection.[25] According to studies, nano-drugs delivered subcutaneously can prolong allograft survival much longer than those administered intravenously, so locally sustained drug delivery might be a viable alternative to intravenous injections. Furthermore, previous studies have found that local drug delivery can alleviate several problems, such as first-pass metabolism and gastrointestinal degradation.[26,27] However, subcutaneous implantation of long-acting systems must be determined whether it can provide sustained drug delivery to treat acute cardiac allograft rejection.

In this study, we explored the potential of microfibers as long-acting systems for the sustained release of highly hydrophobic FK506 in treating acute cardiac allograft rejection. Microfibers were prepared through the blending electrospinning method. Then, we characterized their physical and chemical properties and the sustained release profiles of PCL-FK506 films *in vitro* and the safety of PCL-FK506 *in vivo* using SD rats. Finally, we examined their immunosuppressive effects in a heart transplantation model.

2 Materials and methods

2.1 Materials

FK506 was purchased from MedChem Express (Monmouth Junction, NJ, USA). Polycaprolactone (PCL, MW = 70 kDa–90 kDa) was obtained from the Qingdao Pansi Technology Co., Ltd. Acetone (ACE) and chloroform (DCM) were purchased from Sinopharm Group. 1,1′-Dioctadecyl-3,3,3′,3′-tetramethylindotricarbocyanine iodide (DiR) was purchased from AAT Bioquest (California, USA). All other chemicals used were of analytical grade.

2.2 Preparation of PCL-FK506 microfibers

The electrospinning solution was prepared by dissolving PCL (8 g) and FK506 (80, 160 and 400 mg) in a mixture of solvents DCM and ACE (v/v, 5 : 1) and finally a 40 mL solution (w/v, 20%) was obtained. The resulting solution was pumped through an 18 G blunt needle with a flow rate of 4 mL h^{-1}, and the distance between the fiber collector and syringe was kept within 15 cm. A high voltage of 15 kV and 1 mA current were supplied by a high-voltage power supply (TCM600iP30-30-N, Teslaman, Dalian, China). Humidity and temperature were kept constant at 50% and 25 °C, respectively. PCL/DiR microfibers were prepared in the same manner by adding 100 μL of DiR (10 mg mL^{-1}) to the initial organic mixture.

2.3 Characterization of PCL-FK506

A scanning electron microscope (SEM, Hitachi HT7700, Tokyo, Japan) was used to observe the morphology of PCL-FK506. In order to verify that FK506 has been successfully modified on the surface of PCL, a Fourier transform infrared spectrometer (FTIR, PerkinElmer, USA) was used to detect FK506.[25] Data were collected over the range of 400 to 4000 cm^{-1}. DSC analyses of samples were performed on a DSC2500 (TA Instruments, USA). Samples were typically heated from 20 to 200 °C at 10 °C min^{-1}.

2.4 Drug release from PCL-FK506 microfibers

The sustained release profiles of FK506 from PCL-FK506 microfibers were determined within 14 days using the shaking method. All *in vitro* drug release experiments were performed in a release medium (0.2% Tween solution), as previously reported.[28] In brief, approximately 20 mg of the different PCL-FK506 microfibers were immersed in 40 mL of 0.2% Tween solution in a 50 mL centrifuge tube, respectively. The dissolution study was performed in a shaker incubator at 100 rpm (revolutions per minute) and 37 °C. The FK506 concentration was quantified by high-performance liquid chromatography (HPLC) with a C18 column (4.6 mm × 250 mm, 5 μm) at 40 °C and a mixture of acetonitrile/0.1% phosphoric acid solution in water (70/30, v/v) was adopted as the mobile phase. The flow rate was 1 mL min^{-1}. FK506 was detected at a wavelength of 215 nm. EE and LE were calculated as follows: encapsulation efficiency (%) = (weight of FK506 in PCL/weight of FK506 added) × 100; loading efficiency (%) = (weight of FK506 in PCL/weight of PCL) × 100.

2.5 *In vivo* biodistribution

Male Lewis rats were used to study biodistribution. The rats (n = 3) were implanted with PCL/DiR microfibers subcutaneously. Trafficking of the PCL/DiR microfibers was evaluated using a small animal imaging system (*In vivo* FX PRO, Bruker, USA) equipped with a 750 nm excitation filter and a 790 nm emission filter at POD 1, 4, 7, and 14. The rats were anesthetized before imaging and placed in a dark box in a prone position. The major organs, such as the heart, liver, spleen, lungs and kidneys, were collected and analyzed to evaluate the biodistribution of the PCL/DiR microfibers.

2.6 Heterotopic abdominal heart transplantation and implantation of the PCL-FK506 microfibers

All experiments were carried out using BN and Lewis rats (male, 200–250 g) purchased from Vital River Laboratory (Beijing, China). All animal procedures were performed following the Guidelines for Care and Use of Laboratory Animals of the Huazhong University of Science and Technology and approved by the Animal Ethics Committee of Tongji Medical College, HUST. BN rats and Lewis rats were used as donors

and recipients, respectively. As previously described, heart transplantation was performed using a microsurgical technique.[29] Briefly, the donor rat was anesthetized and heparinized (500 U kg^{-1} i.v.). The superior and inferior vena cava (IVC) and pulmonary veins of the donor's heart were ligated with a 6.0 silk suture, and the ascending aorta and pulmonary artery were sheared with microscopic scissors. The donor's heart was immediately immersed in 4 °C saline. After the abdominal aorta and vena cava were isolated, the donor aorta and pulmonary artery were anastomosed to the recipient's abdominal aorta and IVC using a 9.0 suture. PCL-FK506 membranes were implanted under the skin of the abdomen. The survival time was defined as the complete cessation of heartbeat evaluated by palpation. The cardiac graft that stopped beating within 3 days was excluded from the analysis. The rat heterotopic heart transplantation model was randomized into four groups (n = 6) to analyze the immunosuppressive effect of PCL-FK506.

2.7 Histological staining and immunohistochemical staining

Allografts were harvested at POD 7 or 14 for pathological examination. The samples were fixed in formalin, embedded in paraffin, and stained with hematoxylin and eosin (H&E). Histological evaluation was done according to the criteria of ISHLT.[30] T lymphocyte and macrophage infiltration of the allografts was determined by immunohistochemical staining (IHC) with the anti-CD3 antibody (ab5690, Abcam, Cambridge, UK) and the anti-CD68 antibody (GB11067, Servicebio).

2.8 Flow cytometry and plasma cytokine levels

Blood and inguinal lymph nodes were harvested at POD 7 or 14 for flow cytometric analysis (n = 4–6). Briefly, the blood was collected, and a single-cell suspension was prepared according to the manufacturer's instructions (P8630, Solarbio). The inguinal lymph nodes were dissected from rats and passed through 70 μm filters. Each lymphocyte population was stained with anti-rat CD3-FITC (201403; BioLegend, San Diego, CA), anti-rat CD4-PE (201507; BioLegend, San Diego, CA), anti-rat CD8-APC (201716; BioLegend, San Diego, CA) antibodies. Cells were run on FACSCanto II (BD Biosciences) instrument. Data were analyzed using FlowJo software. The expressions of IL-2 (AF-502-SP, R&D), IL-1β (GB13463, Servicebio) and IL-6 (GB11117, Servicebio) in the allografts were evaluated by immunofluorescence staining at POD 7 and 14. The levels of interleukins (IL)-2 (EK302), IL-6 (EK306), and IL-1β (EK301B) in the plasma were evaluated at POD 7 and 14 by using ELISA kits according to the manufacturer's instructions (Multi Sciences, Hangzhou).

2.9 Statistical analysis

Statistical analysis was performed with Prism8.0 GraphPad software (GraphPad Software, La Jolla, CA). The data are calculated as mean ± standard deviation (SD). The significance of the differences was determined using the Student's t-test or one-way analysis of variance (ANOVA). The survival of cardiac grafts was examined by Kaplan–Meier's analysis. Differences were considered significant for $^{*}P < 0.05$, $^{**}P < 0.01$, and $^{***}P < 0.001$.

3 Results and discussion

3.1 Characterization of materials

PCL-FK506 microfibers were successfully prepared by electrospinning with different amounts of FK506 (1%, 2%, and 5%). A scanning electron microscope (SEM) was employed to observe the morphology of the PCL-FK506 microfibers. As shown in Fig. 1A–D, incorporating FK506 did not impact the morphology. Furthermore, the average diameter of PCL-FK506 microfibers was maintained at 10 μm with uniform morphology, and no drug crystals were visible on the surfaces of PCL-FK506, suggesting that smooth and cylindrical microfibers were successfully produced. In addition, the size was slightly influenced by the addition of FK506. It is reported that precisely controlling the fiber diameter remains a significant obstacle.[31] In our study, there was no significant difference in the diameter and morphology of these PCL-FK506 microfibers. Selected DSC thermograms are shown in Fig. 1E. The melting endotherms for FK506 and PCL are observed at around 127 and 57 °C, respectively. In addition, the endothermic peak of FK506 was also visible in the pattern obtained from the physical mixture of FK506 and PCL. However, such peaks disappear in the PCL-FK506 group. The FTIR spectra of PCL-FK506 are presented in Fig. 1F. The characteristic peaks of FK506 are located at 1630 cm^{-1}, consistent with a previous study.[32] As shown in Fig. 1G and H, the encapsulation efficiency was 97.68 ± 3.46%, 97.68 ± 3.46%, and 95.73 ± 3.90%, respectively. The loading efficiency was 0.97 ± 0.03%, 1.91 ± 0.07%, and 4.79 ± 0.19%, respectively. From these results, it can be concluded that FK506 was successfully encapsulated in PCL.

3.2 Sustained release and degradation performance of PCL-FK506 microfibers *in vitro*

The sustained release profiles and long-term degradation behavior of the PCL-FK506 microfibers within 14 days are presented in Fig. 2. As shown in Fig. 2A, the surface morphology of the degraded samples was observed by SEM on day 1, day 3, day 7, day 10 and day 14, respectively. The results revealed that all the PCL-FK506 microfibers maintained their integrity, and no significant degradation was observed within 14 days. According to the literature, the PCL polymer matrix maintained an intact shape *in vivo* for at least 2 years. It was ultimately excreted through urine and feces.[33] As shown in Fig. 2B, the PCL-FK506 microfibers exhibited a burst release on the first day in three groups. In particular, FK506 release in 1%, 2% or 5% PCL-FK506 microfiber coatings could reach as high as 23.67 ± 2.80%, 31.46 ± 5.10%, and 42.41 ± 0.43% on the first day, respectively, and the PCL-FK506 microfibers containing a higher amount of FK506 exhibited higher burst release. We can see that large-burst drug release is exhibited among the three groups, and this could be attributed to the higher solubility of FK506 in 0.2% Tween solution. The release rate of FK506 slowed down and lasted for about 14 days to reach a plateau. The cumulative release percentages of 1%, 2% or 5% PCL-FK506 microfibers at the end of the drug release experiments were calculated to be 30.72 ± 3.23%, 41.86 ±

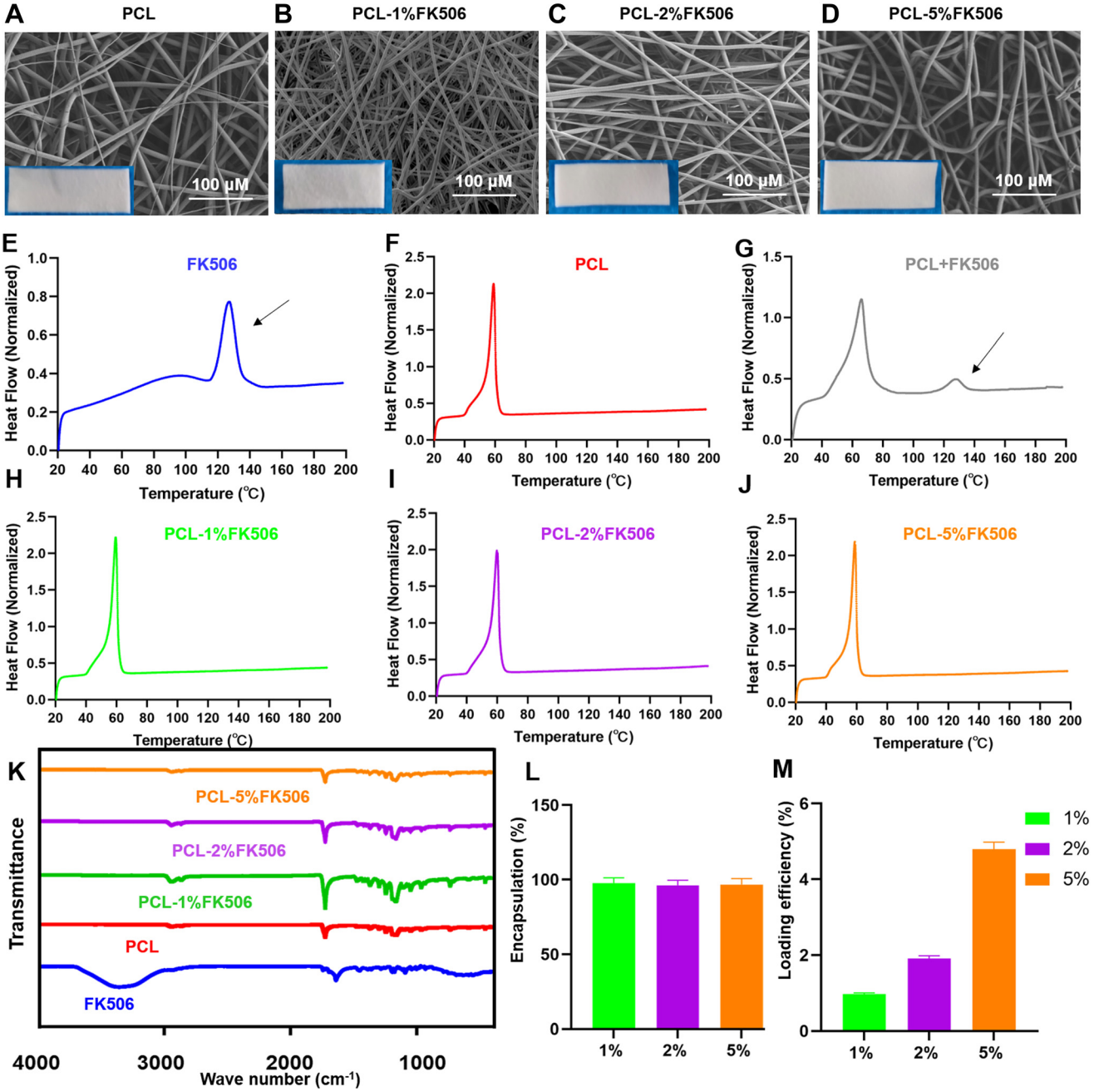

Fig. 1 Characterization of PCL-FK506. (A–D) The physical image and SEM of PCL, PCL-1%FK506, PCL-2%FK506, and PCL-5%FK506. (E–J) DSC and (K) FTIR spectra of FK506, PCL, PCL-1%FK506, PCL-2%FK506, and PCL-5%FK506. (L) FK506 encapsulation and (M) loading efficiency in four groups. Scale bar = 100 μm.

6.00% and 51.78 ± 1.72%, respectively. Therefore, the drug was still released after 14 days. In addition, it may be noted that the amount of released FK506 was higher in 5% PCL-FK506, and the reason may be the increased amount of drug as observed by Dilsiz *et al.*,[34] Saudi *et al.*[35] and Bajpai *et al.*[36] in a similar study. It was reported that the drug release profiles could be divided into three stages. In stages I and II, the drug release is induced by fiber swelling and drug diffusion that dominate the burst release and gentle release. In stage III, the drug release is induced by the degradation of the polymers, which exhibit long-term drug release.[37,38] These data show that PCL-FK506 exhibited long-term release profiles, demonstrating the promise of using this formulation as a long-acting drug delivery system. However, large-burst drug release, uncontrolled duration of drug release and incomplete drug release are still challenging to solve. Therefore, when designing these long-acting drug delivery systems in the future, it is important to consider all contributing factors to obtain the optimal release kinetics to achieve better therapeutic efficacy.[39] Thus, PCL-FK506 microfibers were shown to be a sustainable formulation for long-term drug release.

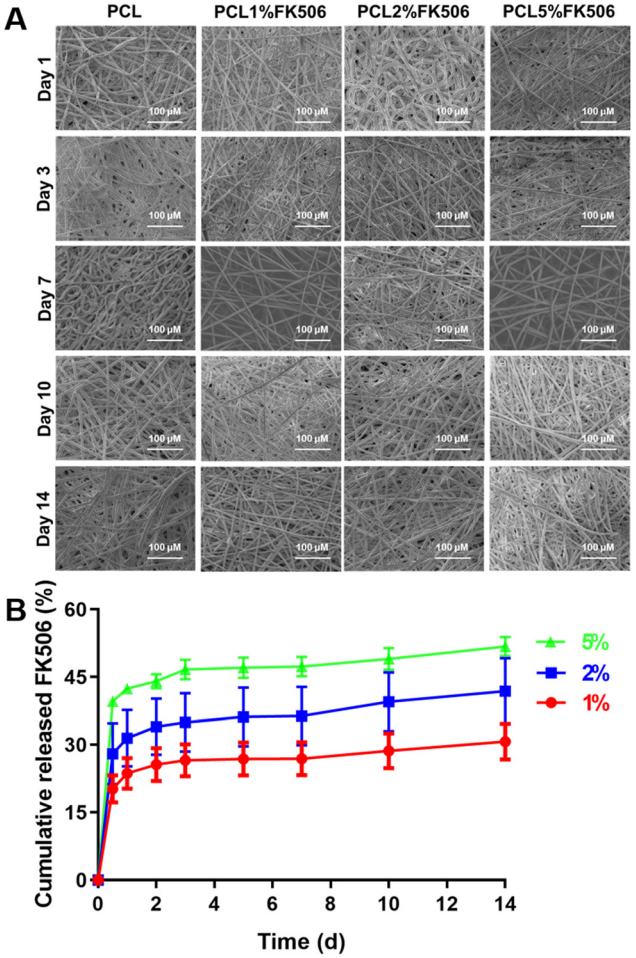

Fig. 2 Sustained release of FK506 *in vitro*. (A) The morphology of PCL, PCL-1%FK506, PCL-2%FK506, and PCL-5%FK506 within 14 days in the release experiment. (B) The *in vitro* release profiles of PCL-1%FK506, PCL-2%FK506, and PCL-5%FK506. Scale bar = 100 μm.

3.3 Biodistribution of fluorescence in organs

In order to simulate PCL-FK506 microfibers' drug release, absorption and metabolism *in vivo*, DiR-labelled PCL microfibers were prepared and subcutaneously implanted on the abdominal skin of each rat. A small animal imaging system was used to evaluate the drug release, absorption and metabolism *in vivo* during 14 days of observation. As shown in Fig. 3A, the results revealed that the fluorescence intensity was mainly accumulated in DiR-labelled PCL microfibers and it gradually decreased from day 1 to day 14. About 50% of the dye was still retained on day 14 of the observation (Fig. 3B). These results demonstrated that DiR loaded in the microfibers could be released sustainably for an extended period *in vivo*. Furthermore, the fluorescence intensity in all the major organs was weak and close to the background level on days 1 and 4 after implantation. Interestingly, the fluorescence intensity was mainly accumulated in the kidneys on days 7 and 14 (Fig. 3C). In addition, DiR-labelled PCL microfibers in all organs had no statistically significant difference after implantation for 14 days (Fig. 3D). These results confirmed that DiR was released from microfibers and then excreted mainly through the kidneys. Nevertheless, the *in vivo* metabolism of DiR might be slightly different from that of FK506, which is metabolized in the liver and excreted *via* bile.[40]

3.4 *In vivo* animal experiments

3.4.1 *In vivo* immunosuppressive effect of PCL-FK506 on day 7. To investigate the effects of PCL-FK506 microfibers on acute cardiac allograft rejection, we implanted the microfibers (PCL-5%FK506) in the region of the abdomen subcutaneously after heart transplantation. Then, the rats received free FK506 (1 mg kg^{-1}, once daily, subcutaneously) or PCL-FK506 microfiber (14 mg kg^{-1}) treatment and were sacrificed on day 7 or 14 after heart transplantation. Next, the PCL-FK506 microfibers and allografts were harvested, sliced, and stained with HE and IHC. The results revealed that the PCL-FK506 microfibers significantly alleviate acute rejection compared with the untreated group. As shown in Fig. 4A, the untreated group exhibited grade 3R rejection as a positive control with massive inflammatory cell infiltration and myocyte necrosis. The PCL-FK506 group revealed only mild inflammatory cell infiltration in most situations and exhibited grade 0R or 1R acute rejection (Fig. 4B). The extent of CD3+ T lymphocyte and CD68+ macrophage infiltration was further assessed in the myocardium using IHC staining. Fig. 4C and E show that the untreated group suffered serious T lymphocyte and macrophage infiltration. In contrast, almost no CD3+ T lymphocyte and CD68+ macrophage infiltration was observed in the PCL-FK506 and free FK506 groups. The quantitative analysis of the CD3+ T lymphocyte (Fig. 4D) and CD68+ macrophage infiltration (Fig. 4F) indicated that both treatment groups effectively inhibit acute rejection in comparison with no treatment group. In recent decades, several treatment options, such as FK506-loaded microspheres[41] and microneedle patches,[42] have been applied to deal with acute rejection in islet and skin transplantation. In this study, sustained release of FK506 also effectively suppressed the intra-graft influxes of T cells and macrophages. Next, we sought to evaluate the lymphocyte in peripheral blood. As shown in Fig. 4G–J, the proportion of CD3+CD4+ T cells in blood was 38.7% ± 1.3% and 28.6% ± 2.6% in the FK506 and PCL-FK506 groups (***$P < 0.001$, n = 4–6 rats per group), respectively. Moreover, the proportion of CD3+CD8+ T cells was 10.5% ± 0.3% and 8.6% ± 0.6% in the FK506 and PCL-FK506 groups (**$P < 0.01$, n = 4–6 rats per group), respectively. Remarkably, the CD4+ and CD8+ effector T cells in peripheral blood were more effectively suppressed by PCL-FK506 microfibers than the free FK506 treatment. This phenomenon may be related to the massive release of FK506 by PCL-FK506 microfibers in the early stage, when a large amount of FK506 was absorbed into the blood, resulting in a high concentration of FK506 in the blood and strongly inhibiting the proliferation and activation of effector T cells. Furthermore, the proportion of CD3+CD4+ and CD3+CD8+ T cells in the inguinal lymph nodes was assessed. As shown in Fig. 4K–N, the proportion of CD3+CD4+ T cells was 45.9% ±

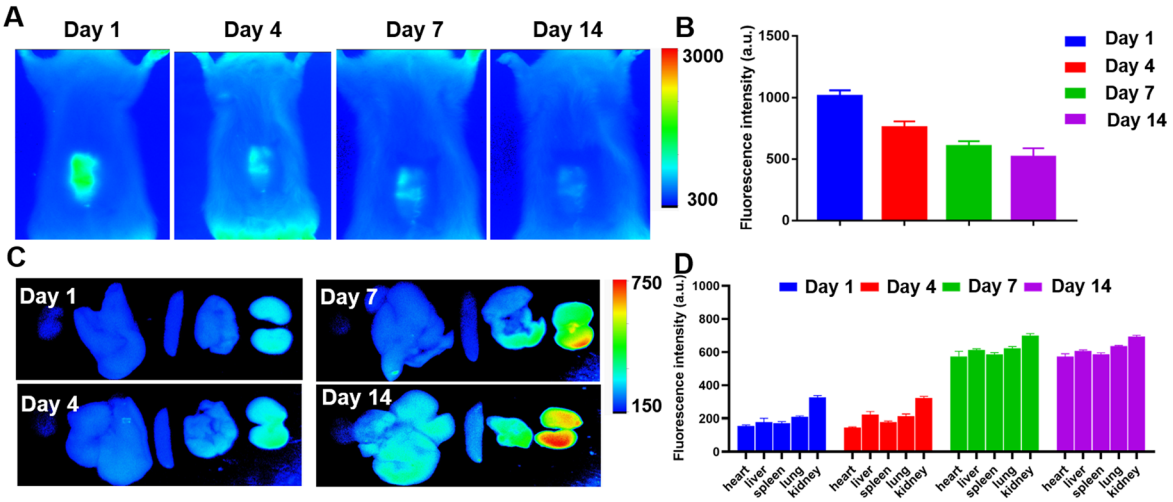

Fig. 3 Biodistribution of DiR-labeled PCL within 14 days. (A) *In vivo* images of DiR-labelled PCL on day 1, day 3, day 7 and day 14. (B) Quantitative analysis of the fluorescence intensity. (C) *Ex vivo* fluorescence images of the major organs on day 1, day 3, day 7 and day 14. (D) Quantitative analysis of the fluorescence intensity.

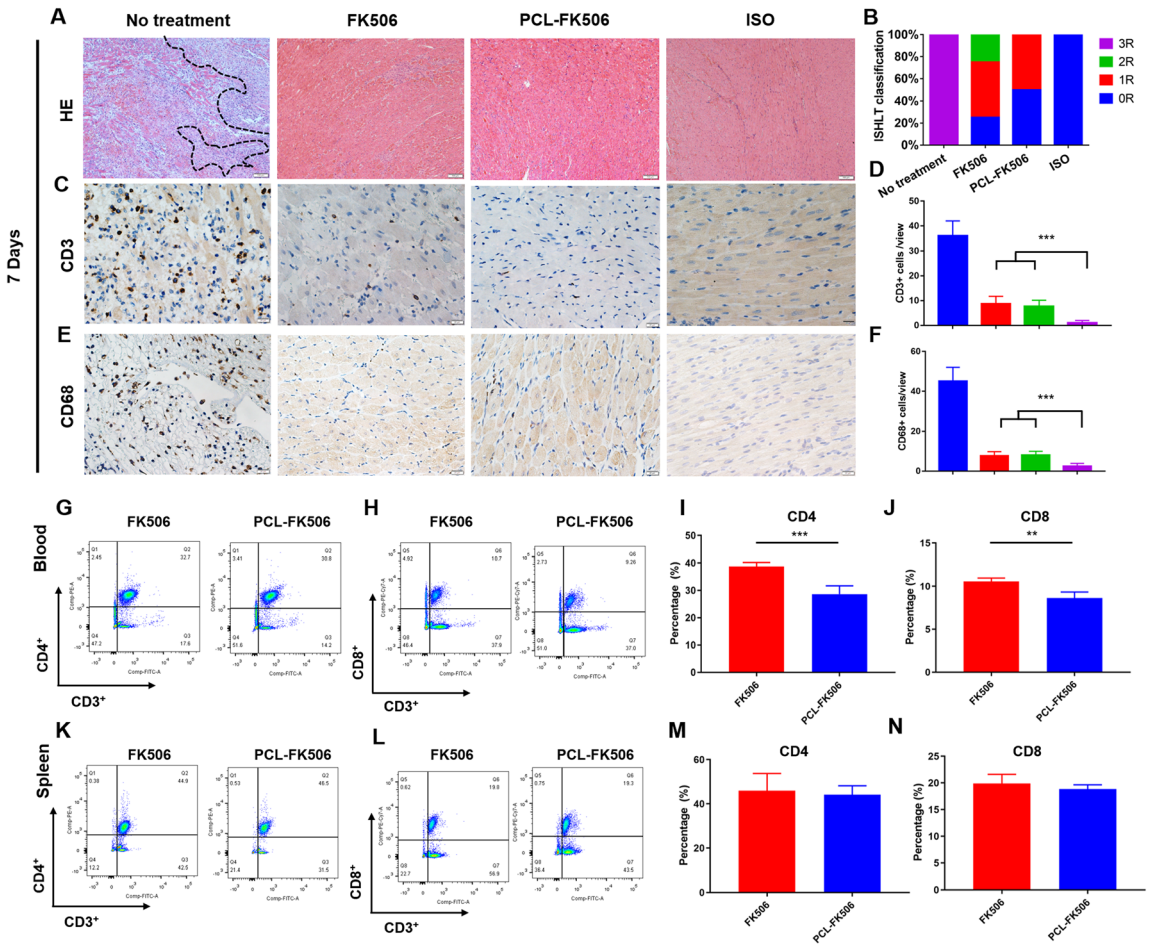

Fig. 4 Immunosuppressive effects of PCL-FK506 on the cardiac allograft on POD 7. (A) H&E staining of the allograft tissue sections, scale bar = 100 μm and (B) grade of the allograft tissues evaluated on POD 7. (C) Immunohistochemical staining with CD3 T lymphocytes and (E) CD68 macrophages in allograft tissues, scale bar = 20 μm. (D–F) Quantification analysis of the number of lymphocytes and macrophages in the allograft tissues. FACS analysis of CD3+CD4+ (G and H) and CD3+CD8+ (I and J) lymphocytes in blood and inguinal lymph nodes (K–N) from heart transplant recipients treated with free FK506 and PCL-FK506 (n = 4–6). $^{**}P < 0.01$, and $^{***}P < 0.001$.

6.7% and 44.1% ± 3.5% in the FK506 and PCL-FK506 groups (n = 4–6 rats per group), respectively. Moreover, the proportion of CD3+CD8+ T cells was 19.9% ± 1.5% and 18.8% ± 0.7% in the FK506 and PCL-FK506 groups (n = 4–6 rats per group), respectively. Notably, there is no significant difference between the FK506 and PCL-FK506 groups in terms of the proportion of CD4+ and CD8+ effector T cells in the inguinal lymph node. The results indicated that both treatment groups effectively suppressed the number of effector T cells in the lymph nodes.

3.4.2 *In vivo* immunosuppressive effects of PCL-FK506 on day 14. To test the long-term immunosuppressive effects of PCL-FK506, the histology of the grafts and the levels of effector T cells in the graft tissues, blood and lymph nodes were evaluated on POD 14. As shown in Fig. 5A and B, the PCL-FK506 group revealed only mild lymphocyte infiltration in most situations and exhibited grade 0R or 1R acute rejection on POD 14. The extent of CD3+ T lymphocyte and CD68+ macrophage infiltration was further assessed in the myocar-

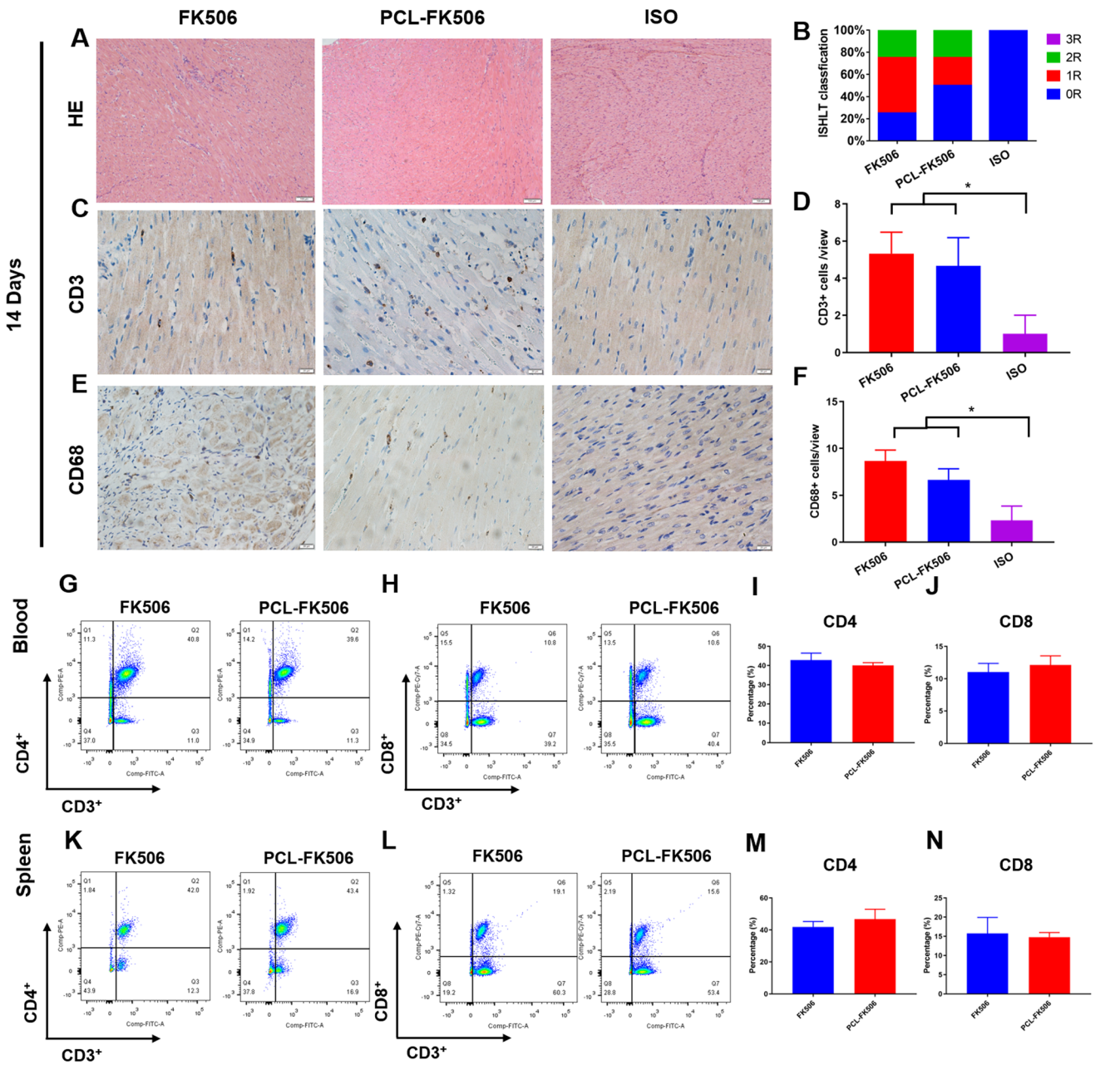

Fig. 5 Immunosuppressive effects of PCL-FK506 on the cardiac allograft on POD 14. (A) H&E staining of the allograft tissue sections, scale bar = 100 μm and (B) grade of the allograft tissues evaluated on POD 7. (C) Immunohistochemical staining with CD3 T lymphocytes and (E) CD68 macrophages in allograft tissues, scale bar = 20 μm. (D–F) Quantification analysis of the number of lymphocytes and macrophages in the allograft tissues. FACS analysis of CD3+CD4+ (G and H) and CD3+CD8+ (I and J) lymphocytes in blood and inguinal lymph nodes (K–N) from heart transplant recipients treated with free FK506 and PCL-FK506 (n = 4–6). *P < 0.05.

dium using immunohistochemical staining (Fig. 5C–F). Fig. 5C and E show that there was only mild CD3+ T lymphocyte and CD68+ macrophage infiltration in the PCL-FK506 group and free FK506 group compared with the ISO group. The quantitative analysis of the CD3+ T lymphocyte (Fig. 5D) and CD68+ macrophage infiltration (Fig. 5F) indicated that PCL-FK506 microfibers effectively inhibit acute rejection for up to 14 days and maintain acute rejection at a low level compared with the ISO group. As shown in Fig. 5G and I, the proportion of CD3+CD4+ T cells was 42.9% ± 3.1% and 40.0% ± 1.3% in the FK506 and PCL-FK506 groups (n = 4–6 rats per group), respectively. Moreover, the results in Fig. 5H and J show that the proportion of CD3+CD8+ T cells was 11.0% ± 1.2% and 12.1% ± 1.2% in the FK506 and PCL-FK506 groups (n = 4–6 rats per group), respectively. To further evaluate the immune response in inguinal lymph nodes, we assessed the proportion of CD3+CD4+ and CD3+CD8+ T cells. As shown in Fig. 5K and M, the proportion of CD3+CD4+ T cells was 41.9% ± 2.9% and 46.7% ± 5.4% in the FK506 and PCL-FK506 groups (n = 4–6 rats per group), respectively. Moreover, as shown in Fig. 5L and N, the proportion of CD3+CD8+ T cells was 14.0% ± 3.6% and 14.3% ± 1.1% in the FK506 and PCL-FK506 groups (n = 4–6 rats per group), respectively. Notably, there is no significant difference between the FK506 and PCL-FK506 groups in terms of the proportion of CD4+ and CD8+ effector T cells in the inguinal lymph node. These results indicated that PCL-FK506 microfibers effectively inhibited the proliferation of effector T cells as free FK506 treatment did on POD 14. We think it may be related to the effective concentration of FK506 in the inguinal lymph node, which is accumulatively released from PCL-FK506 microfibers locally, and it was previously described in similar studies.[43,44]

3.5 Secretion of cytokines in serum and allograft tissues

According to the literature, the cytokines interleukin-2 (IL-2), IL-1β and IL-6 have been suggested as indicators of an anti-graft immune response.[45,46] Hence, the expressions of IL-2, IL-1β and IL-6 in the allografts were evaluated by immunofluorescence staining on POD 7 and 14 after heart transplantation. Interestingly, there is no significant difference in the expression level of IL-2, IL-1β, and IL-6 among the free FK506, PCL-FK506 and the ISO groups on POD 7 (Fig. 6A–C). Furthermore, the expression levels of pro-inflammatory cytokines in the serum of rats were detected by ELISA on POD 7 and 14 after free FK506 and PCL-FK506 treatment. On POD 7, no difference was noted in the levels of IL-2, IL-1β and IL-6 among the treatment groups (Fig. 6D). It is worth noting that with the treatment of PCL-FK506 14 days after heart transplantation, the expressions of IL-2, IL-6 and IL-1β in the allografts remained at a low level compared with the ISO group (Fig. 7A–C). Moreover, the results in Fig. 7D revealed that higher levels of inflammatory cytokines IL-2 and IL-1β were observed in the free FK506 treatment group in comparison with those of the PCL-FK506 group on POD 14 (free FK506

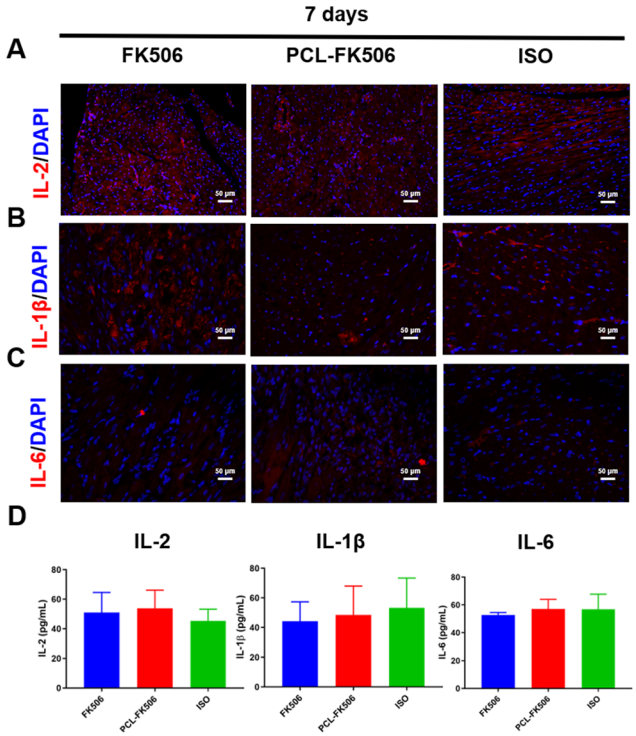

Fig. 6 Secretion of cytokines in the allografts and serum on POD 7. Immunofluorescence staining of IL-2 (A), IL-β (B), and IL-6 (C) secretion in allografts. (D) The concentrations of IL-2, IL-β, and IL-6 in serum. Each value represents the mean ± SD (n = 4–6). Scale bar = 50 μm.

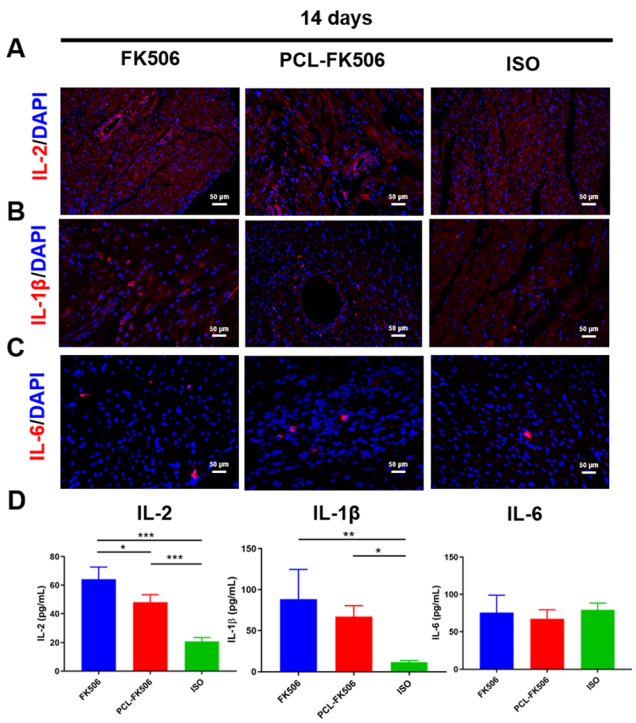

Fig. 7 Secretion of cytokines in the allografts and serum on POD 14. Immunofluorescence staining of IL-2 (A), IL-β (B), and IL-6 (C) secretion in allografts. (D) The concentrations of IL-2, IL-β, and IL-6 in serum. Each value represents the mean ± SD (n = 4–6). *P < 0.05, **P < 0.01, and ***P < 0.001. Scale bar = 50 μm.

vs. PCL-FK506: 64.23 ± 7.32 *vs.* 48.05 ± 4.67 pg mL^{-1} for IL-2 and 88.29 ± 31.47 *vs.* 67.08 ± 11.57 for IL-1β, $^{*}P < 0.05$, $^{***}P < 0.001$, $n = 4$ rats per group). However, there is no significant difference in the level of IL-6 among the three groups. The results demonstrated that inflammatory cytokines were effectively suppressed in the free FK506 and PCL-FK506 groups on POD 7, and PCL-FK506 treatment exhibited better therapeutic outcomes on POD 14. Taken together, the PCL-FK506 microfibers maintain the immunosuppressive functions of FK506, reducing the expression of inflammatory cytokines and improving the prognosis of heart transplantation.

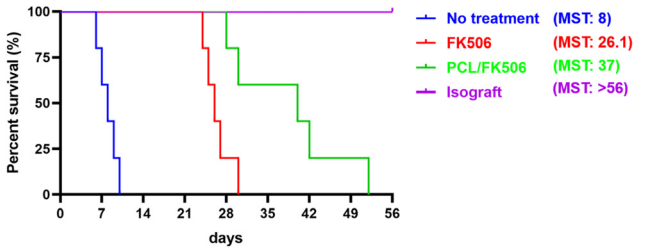

Fig. 8 Kaplan–Meier's survival curves of the cardiac allograft treated with FK506 and PCL-FK506 ($n = 6$).

3.6 PCL-FK506 prolongs cardiac transplant survival

To further evaluate the effects of PCL-FK506 microfibers in long-term allograft survival, Lewis rats that underwent transplantation were treated with free FK506 (1 mg kg^{-1}) from day 1 to day 14 or subcutaneous implantation of PCL-FK506 microfibers (14 mg kg^{-1}) after heart transplantation, respectively. The control groups were no treatment group and the ISO group. As shown in Fig. 8, we observed a significant prolongation of cardiac transplant survival following treatment with PCL-FK506 microfibers (mean survival time of untreated control recipients, free FK506, PCL-FK506 and negative control recipients was 8, 26.1, 37, and >56 days, respectively, $n = 6$ rats per group). It was noted that about 50% of the allografts in the PCL-FK506-treated group survived more than 40 days. Our data indicate that the treatment with PCL-FK506 microfibers significantly prolonged the cardiac allograft survival time compared with that with FK506 alone (PCL-FK506 *vs.* free FK506: 37 *vs.* 26.1 days). Therefore, PCL-FK506 microfibers exhibited a better therapeutic efficacy than free FK506 treatment. In this regard, multiple studies have reported that topical application of FK506 microspheres effectively prevented acute rejection and prolonged the survival time in vascularized composite allotransplantation and islet transplantation.[41,43,47] To the best of our knowledge, it is the first time that PCL-FK506 microfibers, as a robust long-acting

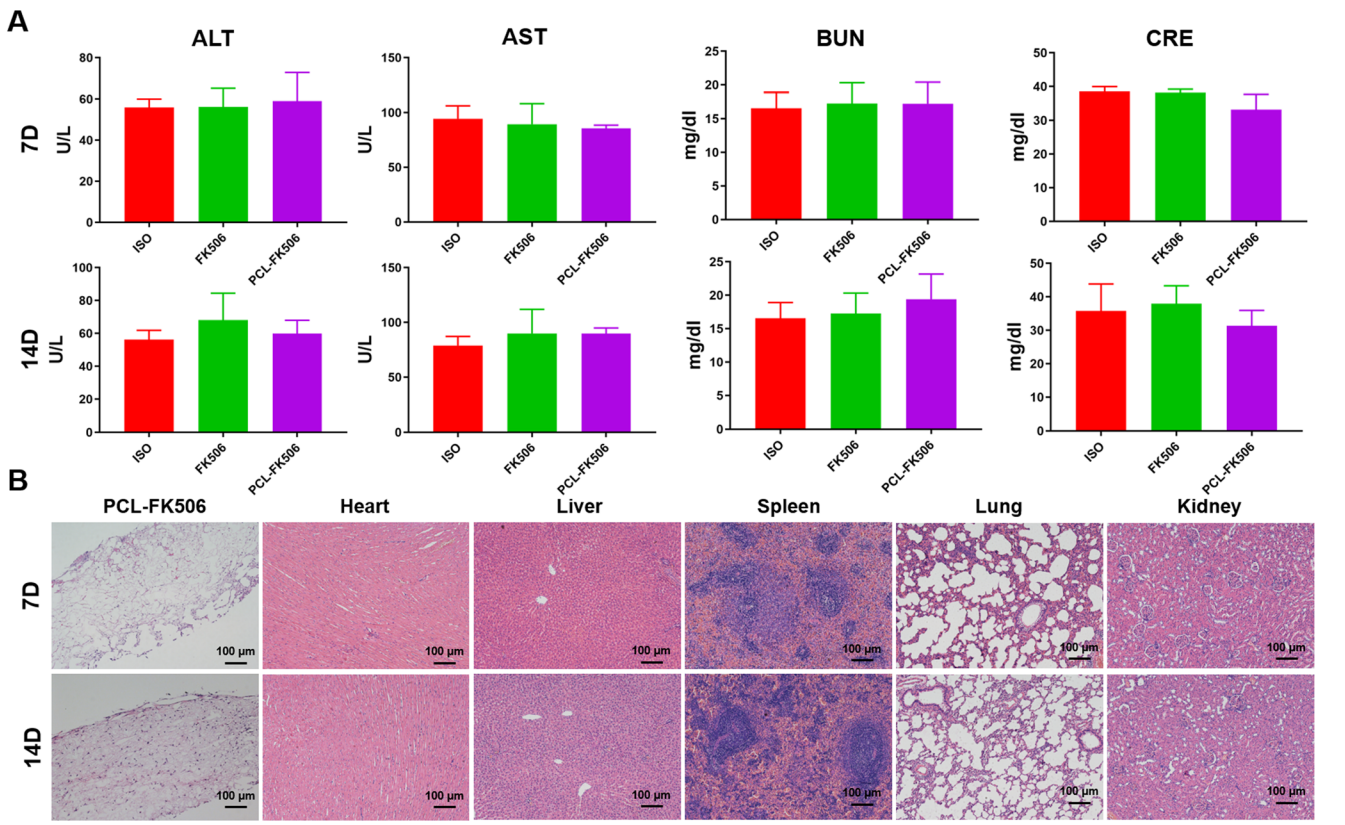

Fig. 9 *In vivo* toxicity evaluation of PCL-FK506. (A) Serum levels of AST, ALT, BUN, and CRE. (B) H&E staining of PCL-FK506 and the major organs. Each value represents the mean ± SD ($n = 3$). Scale bar = 100 μm.

FK506 delivery system, effectively prevented acute rejection and extended the survival time beyond 30 days in heart transplantation. Hence, we believe that this new approach may be a safe and effective way to treat acute rejection in the future in heart transplantation.

3.7 *In vivo* biocompatibility evaluation

Subcutaneous implantation of the PCL-FK506 microfibers into SD rats was carried out to evaluate *in vivo* compatibility. 7 days and 14 days after implantation, the implants and the major organs were removed and sectioned for H&E staining. Furthermore, the toxicity of implants was assessed by measuring the liver and kidney function indicators, such as alanine aminotransferase (ALT), aspartate aminotransferase (AST), blood urine nitrogen (BUN), and creatinine (CRE). As shown in Fig. 9A, there was no significant difference among these groups. These results indicate that subcutaneous implantation of the long-acting sustained-release microfibers does not cause liver and kidney toxicity. Moreover, the histology analysis revealed no toxicity differences among the major organs, and there is almost no infiltration of inflammatory cells in PCL-FK506 microfibers (Fig. 9B).

4 Conclusion

In summary, we have developed a long-acting drug delivery system and achieved adequate immunosuppression in a heart transplantation model. Our results indicated that the subcutaneous implantation of biodegradable PCL-FK506 represents an effective, safe and simple method to achieve adequate immunosuppression in organ transplantation. We proposed that this drug delivery approach would be suitable for developing long-lasting immunomodulatory agents that safely and effectively prolong cardiac graft survival.

Author contributions

M. X. X. and L. Z.: conceptualization and investigation. C. D., J. X., W. P. F., M. R. H., L. L. X., and Y. S. S.: methodology, software, validation, and writing. W. Y. W., L. Y. Y., Y. H. C., and T. G.: visualization and investigation. Q. F. J., J. W., Q. L., and Y. L. Y.: supervision and writing – reviewing and editing. All authors have given approval to the final version of the manuscript.

Conflicts of interest

The authors have no conflicts of interest to declare.

Acknowledgements

The authors would like to acknowledge funding from the National Nature Science Foundation of China (no. 81922033, 81727805, 81801716, and 81801715) and the Shenzhen Science and Technology under grants SGDX20190917094601717 and JCYJ20210324141216040.

References

1 J. Stehlik, J. Kobashigawa, S. A. Hunt, H. Reichenspurner and J. K. Kirklin, *Circulation*, 2018, **137**, 71–87.
2 T. Hussain, K. Nassetta, L. C. O'Dwyer, J. E. Wilcox and S. M. Badawy, *Transplant. Rev.*, 2021, **35**, 100651.
3 W. Li, J. Tang, D. Lee, T. R. Tice, S. P. Schwendeman and M. R. Prausnitz, *Nat. Rev. Mater.*, 2022, **7**, 406–420.
4 P. Agarwal and I. D. Rupenthal, *Drug Discovery Today*, 2013, **18**, 337–349.
5 Y. Shi, A. Lu, X. Wang, Z. Belhadj, J. Wang and Q. Zhang, *Acta Pharm. Sin. B*, 2021, **11**, 2396–2415.
6 S. A. Krovi, L. M. Johnson, E. Luecke, S. L. Achilles and A. van der Straten, *Adv. Drug Delivery Rev.*, 2021, **176**, 113849.
7 Y. Chang, J. Jiang, W. Chen, W. Yang, L. Chen, P. Chen, J. Shen, S. Qian, T. Zhou, L. Wu, L. Hong, Y. Huang and F. Li, *Appl. Mater. Today*, 2020, **18**, 100492.
8 Y. R. Carriles, M. Suetel, S. Henze, R. Álvarez Brito and W. D. Mueller, *Int. J. Pharm.*, 2021, **606**, 120735.
9 Z. Yue, B. Hu, Z. Chen, G. Zheng, Y. Wang, C. Yang, P. Cao, X. Wu, L. Liang, F. Zang, J. Wang, J. Li, T. Zhang, J. Wu and H. Chen, *Mater. Today Bio*, 2022, **17**, 100469.
10 S. Wu, T. Dong, Y. Li, M. Sun, Y. Qi, J. Liu, M. A. Kuss, S. Chen and B. Duan, *Appl. Mater. Today*, 2022, **27**, 101473.
11 P. Wen, Y. Wen, M. H. Zong, R. J. Linhardt and H. Wu, *J. Agric. Food Chem.*, 2017, **65**, 9161–9179.
12 Z. Gu, H. Yin, J. Wang, L. Ma, Y. Morsi and X. Mo, *Colloids Surf., B*, 2018, **161**, 331–338.
13 H. Cheng, X. Yang, X. Che, M. Yang and G. Zhai, *Mater. Sci. Eng., C*, 2018, **90**, 750–763.
14 X. Hu, S. Liu, G. Zhou, Y. Huang, Z. Xie and X. Jing, *J. Controlled Release*, 2014, **185**, 12–21.
15 J. Liu, T. Li, H. Zhang, W. Zhao, L. Qu, S. Chen and S. Wu, *Mater. Today. Bio*, 2022, **14**, 100243.
16 B. W. Walker, R. P. Lara, C. H. Yu, E. S. Sani, W. Kimball, S. Joyce and N. Annabi, *Biomaterials*, 2019, **207**, 89–101.
17 L. Li, G. J. Gatto, R. M. Brand, S. A. Krovi, M. L. Cottrell, C. Norton, A. van der Straten and L. M. Johnson, *J. Controlled Release*, 2021, **340**, 188–199.
18 X. He, Z. Huang, W. Liu, Y. Liu, H. Qian, T. Lei, L. Hua, Y. Hu, Y. Zhang and P. Lei, *Colloids Surf., B*, 2021, **204**, 111825.
19 M. C. Souza, S. L. Fialho, P. A. Souza, G. O. Fulgêncio, G. R. Da Silva and A. Silva-Cunha, *Curr. Eye Res.*, 2014, **39**, 99–102.
20 M. Sun, Y. Liu, K. Jiao, W. Jia, K. Jiang, Z. Cheng, G. Liu and Y. Luo, *J. Mater. Chem. B*, 2022, **10**, 765–778.
21 Y. Huang, R. Shi, M. Gong, J. Zhang, W. Li, Q. Song, C. Wu and W. Tian, *Int. J. Nanomed.*, 2018, **13**, 4831–4844.

22 Y. Fu, X. Li, Z. Ren, C. Mao and G. Han, *Small*, 2018, **14**, 1801183.
23 S. Chen, R. Li, X. Li and J. Xie, *Adv. Drug Delivery Rev.*, 2018, **132**, 188–213.
24 L. Zhao, M. Orlu and G. R. Williams, *Int. J. Pharm.*, 2021, **599**, 120426.
25 C. Deng, Q. Jin, Y. Wu, H. Li, L. Yi, Y. Chen, T. Gao, W. Wang, J. Wang, Q. Lv, Y. Yang, J. Xu, W. Fu, L. Zhang and M. Xie, *Drug Delivery*, 2021, **28**, 1759–1768.
26 F. Qu, R. Geng, Y. Liu and J. Zhu, *Theranostics*, 2022, **12**, 3372–3406.
27 S. A. Ali, N. A. Alhakamy, K. M. Hosny, E. Alfayez, D. M. Bukhary, A. Y. Safhi, M. Y. Badr, R. Y. Mushtaq, M. Alharbi, B. Huwaimel, M. Alissa, S. Alshehri, A. H. Alamri and T. Alqahtani, *Drug Delivery*, 2022, **29**, 2773–2783.
28 C. Deng, Y. Chen, L. Zhang, Y. Wu, H. Li, Y. Wu, B. Wang, Z. Sun, Y. Li, Q. Lv, Y. Yang, J. Wang, Q. Jin and M. Xie, *Int. J. Pharm.*, 2019, **575**, 118951.
29 K. Ono and E. S. Lindsey, *J. Thorac. Cardiovasc. Surg.*, 1969, **57**, 225–229.
30 S. Stewart, G. L. Winters, M. C. Fishbein, H. D. Tazelaar, J. Kobashigawa, J. Abrams, C. B. Andersen, A. Angelini, G. J. Berry, M. M. Burke, A. J. Demetris, E. Hammond, S. Itescu, C. C. Marboe, B. McManus, E. F. Reed, N. L. Reinsmoen, E. R. Rodriguez, A. G. Rose, M. Rose, N. Suciu-Focia, A. Zeevi and M. E. Billingham, *J. Heart Lung Transplant.*, 2005, **24**, 1710–1720.
31 X. Feng, J. Li, X. Zhang, T. Liu, J. Ding and X. Chen, *J. Controlled Release*, 2019, **302**, 19–41.
32 S. Pathak, S. Regmi, B. Gupta, B. K. Poudel, T. T. Pham, C. S. Yong, J. O. Kim, J. R. Kim, M. H. Park, Y. K. Bae, S. Yook, C. H. Ahn and J. H. Jeong, *Drug Delivery*, 2017, **24**, 1350–1359.
33 H. Sun, L. Mei, C. Song, X. Cui and P. Wang, *Biomaterials*, 2006, **27**, 1735–1740.
34 S. M. Eskitoros-Togay, Y. E. Bulbul, S. Tort, F. D. Korkmaz, F. Acarturk and N. Dilsiz, *Int. J. Pharm.*, 2019, **565**, 83–94.
35 S. Saudi, S. R. Bhattarai, U. Adhikari, S. Khanal, J. Sankar, S. Aravamudhan and N. Bhattarai, *Nanoscale*, 2020, **12**, 23556–23569.
36 S. K. Bajpai, M. Jadaun, M. Bajpai, P. Jyotishi, F. F. Shah and S. Tiwari, *Int. J. Biol. Macromol.*, 2017, **104**, 1064–1071.
37 J. Wu, Z. Zhang, J. Gu, W. Zhou, X. Liang, G. Zhou, C. C. Han, S. Xu and Y. Liu, *J. Controlled Release*, 2020, **320**, 337–346.
38 S. R. Benhabbour, M. Kovarova, C. Jones, D. J. Copeland, R. Shrivastava, M. D. Swanson, C. Sykes, P. T. Ho, M. L. Cottrell, A. Sridharan, S. M. Fix, O. Thayer, J. M. Long, D. J. Hazuda, P. A. Dayton, R. J. Mumper, A. D. M. Kashuba and J. V. Garcia, *Nat. Commun.*, 2019, **10**, 4324.
39 G. Liu, Z. Gu, Y. Hong, L. Cheng and C. Li, *J. Controlled Release*, 2017, **252**, 95–107.
40 M. A. Sikma, E. M. van Maarseveen, E. A. van de Graaf, J. H. Kirkels, M. C. Verhaar, D. W. Donker, J. Kesecioglu and J. Meulenbelt, *Am. J. Transplant.*, 2015, **15**, 2301–2313.
41 T. T. Nguyen, C. D. Phung, J. O. Kim, C. S. Yong, J. R. Kim, S. Yook and J. H. Jeong, *J. Controlled Release*, 2021, **336**, 274–284.
42 N. Puigmal, P. Dosta, Z. Solhjou, K. Yatim, C. Ramírez, J. Y. Choi, J. B. Alhaddad, A. P. Cosme, J. Azzi and N. Artzi, *Adv. Funct. Mater.*, 2021, **31**, 2100128.
43 J. V. Unadkat, J. T. Schnider, F. G. Feturi, W. Tsuji, J. M. Bliley, R. Venkataramanan, M. G. Solari, K. G. Marra, V. S. Gorantla and A. M. Spiess, *Plast. Reconstr. Surg.*, 2017, **139**, 403e–414e.
44 R. Kojima, T. Yoshida, H. Tasaki, H. Umejima, M. Maeda, Y. Higashi, S. Watanabe and N. Oku, *Int. J. Pharm.*, 2015, **492**, 20–27.
45 S. C. Jordan, N. Ammerman, J. Choi, S. Kumar, E. Huang, M. Toyoda, I. Kim, G. Wu and A. Vo, *Transplantation*, 2020, **104**, 2497–2506.
46 M. C. Deng, M. Erren, L. Kammerling, F. Gunther, S. Kerber, A. Fahrenkamp, G. Assmann, G. Breithardt and H. H. Scheld, *Transplantation*, 1995, **60**, 1118–1124.
47 J. D. Fisher, S. C. Balmert, W. Zhang, R. Schweizer, J. T. Schnider, C. Komatsu, L. Dong, V. E. Erbas, J. V. Unadkat, A. M. Aral, A. P. Acharya, Y. Kulahci, H. R. Turnquist, A. W. Thomson, M. G. Solari, V. S. Gorantla and S. R. Little, *Proc. Natl. Acad. Sci. U. S. A.*, 2019, **116**, 25784–25789.

